Chemical Journal of Kazakhstan
Volume 2, Number 78(2022), 119-131 https://doi.org/10.51580/2022-2/2710-1185.71

УДК 544.653.3+546.57

ELECTROCATALYTIC HYDROGENATION OF *P*- AND *O*-ISOMERS OF NITROBENZOIC ACID USING BIMETALLIC FE-AG COMPOSITES

***Soboleva Ye.A.*[1*], *Vissurkhanova Ya.A.*[1,2], *Ivanova N.M.*[1],**
***Beisenbekova M.E.*[1], *Kenzhetayeva S.O.*[2]**

[1]*Institute of Organic Synthesis and Chemistry of Coal of the Republic of Kazakhstan LLP,*
Karaganda, Kazakhstan
[2] *NPJSC Ye.A. Buketov Karaganda State University, Kazakhstan*
[*]*E-mail: esoboleva-kz@mail.ru*

Abstract: Bimetallic Fe-Ag composites were fabricated based on silver (I) ferrite ($AgFeO_2$) synthesized using a co-precipitation method with and without the polyvinyl alcohol as a nanoparticle stabilizer, followed by the heat treatment at 500, 700 and 900°C and electrochemical reduction. Phase compositions and morphological features of $AgFeO_2$ samples produced after heat treatment and after electrochemical experiments were determined by X-ray diffraction analysis and electron microscopy. A decrease in the temperature of the thermal decomposition of silver ferrite prepared with polyvinyl alcohol was established. The possibility of the electrochemical reduction of $AgFeO_2$ in aqueous alkaline catholyte on a copper cathode with the formation of crystalline phases of both metals or their alloy was shown. The Fe-Ag composites formed during heat treatment and electrochemical reduction were used as electrocatalysts in the electrohydrogenation of *p*- and *o*-isomers of nitrobenzoic acid and exhibited high activity. Compared to their electrochemical reduction under similar conditions, the hydrogenation rate and hydrogen utilization coefficient were increased, and their conversion reached the maximum values. The main products of electrocatalytic hydrogenation are *p*- and *o*-isomers of aminobenzoic acid, which are widely used in the production of drugs (for example, benzocaine, novocaine., etc.).

Key words: bimetallic Fe-Ag composites, silver ferrite, polymer stabilizer, electrocatalytic hydrogenation, *p*- and *o*-isomers of nitrobenzoic acid

Soboleva Yelena Anatol’evna	*Candidate of chemical science, e-mail: esoboleva-kz@mail.ru, ORCID: https://orcid.org/0000-0002-1089-367X*
Vissurkhanova Yakha Amkhadovna	*PhD student, e-mail: yakhavisurkhanova@bk.ru, ORCID: https://orcid.org/0000-0001-7279-1145*
Ivanova Nina Mikhailovna	*Doctor of Chemical Sciences, Professor, e-mail: nmiva@mail.ru, ORCID: https://orcid.org/0000-0001-8564-8006*
Beisenbekova Moldir Erbolatovna	*Bachelor of Engineering and Technology, e-mail: monika_99@list.ru, ORCID: https://orcid.org/0000-0002-4156-2259*
Kenzhetayeva Saule Orynbayevna	*candidate of chemical science, Professor, e-mail: kenzhetaeva58@mail.ru, ORCID: https://orcid.org/0000-0003-1891-5236*

Citation: Soboleva Ye.A.**,** Vissurkhanova Ya.A.**,** Ivanova N.M., Beisenbekova M.E., Kenzhetaeva S.O. Electrocatalytic hydrogenation of *p*- and *o*-isomers of nitrobenzoic acid using bimetallic Fe-Ag composites. *Chem. J. Kaz.*, **2022**, *2(78),* 119-131. DOI: https://doi.org/10.51580/2022-2/2710-1185.71

1. Introduction

Nanoparticles of a number of metal ferrites with magnetic properties are used as catalysts in various reactions of organic chemistry [1]. This group of metal ferrites also includes silver (I) ferrite, $AgFeO_2$, which exhibits high photocatalytic activity in many chemical processes [2–4]. In addition, silver ferrites are widely employed as sensors, energy storage devices, in lithium-ion batteries, and for water purification due to their non-toxicity, optical, electrical and magnetic properties, as well as a unique electronic structure [5-7]. It is known [8] that silver (I) ferrite has a delafossite-type layered structure with the general chemical formula ABO_2, which is characterized by alternating layers of BO_6 octahedra with common edges, where the B cation can include various trivalent transition metal cations (for example, Fe^{3+}) with close-packed monovalent A^+ metal cations, which are located between the layers. For $AgFeO_2$, rhombohedral (space group symmetry R-3m) and hexagonal (space group symmetry P63/mmc) crystal structures are known [9].

In literature, various methods for producing stable nanosized particles of silver ferrite have outlined: sol-gel method [2], hydrothermal [10], co-precipitation [11], solid-phase synthesis [12] and others. These methods can be used to prepare silver ferrite with a highly crystalline structure, with good dispersion and stability, with the ability to control the size and shape of its particles [13-15]. It is known that silver has antibacterial properties, and recently a tendency to obtain mixed ferrites of metals with silver has been developed to create new composite materials with good physical properties and antimicrobial activity [16, 17], which can be promising in biomedical and pharmaceutical productions.

Some metal ferrites, in addition to their direct use as catalysts, serve as sources for preparing nano- and microparticles of bimetallic iron-containing composites, which also have catalytic properties. The scientific papers [18-20] describe in more detail the creation of Fe-Cu- and Fe-Zn-composites by thermal reduction of metal ferrites in a hydrogen flow or in an environment of other reducing gases. We have also shown that as a result of the electrochemical reduction of copper (II) ferrite ($CuFe_2O_4$) the Fe–Cu composites are formed with various metal contents determined by the temperature of their preliminary heat treatment, and they exhibit high electrocatalytic activity [21]. Nickel and zinc ferrites behave somewhat differently under similar conditions [22, 23].

This paper presents the investigations of the thermal and electrochemical reduction of silver ferrite, the preparation of Fe-Ag composites on its basis, and their application in the electrohydrogenation of nitrobenzoic acid (NBA) isomers, the amino-products of which are intermediate reagents in the synthesis of known drugs (benzocaine, novocaine, dicaine and etc.).

It should be noted that there are practically no studies on the thermal and electrochemical reduction of silver ferrite in the literature. At the same time, it is known [7, 24] that at temperatures of 600-700°C, silver ferrite decomposes with the loss of oxygen and the formation of metallic silver and Fe_2O_3:

$$4AgFeO_2 \rightarrow 4Ag + 2Fe_2O_3 + O_2. \qquad (1)$$

In addition, there are studies on the creation of bimetallic Fe–Ag nanoparticles and investigation of their optical, magnetic, photocatalytic, and catalytic properties [25–27]. Their syntheses are based mainly on the chemical reduction of silver cations in the presence of iron or its oxides and the formation of core-in-shell nanoparticles. For example, in [25], at the first stage of syntheses, Fe and Fe_3O_4 nanoparticles were first prepared by the hydrothermal method, then, in their presence, silver cations were reduced from its nitrate using sodium borohydride, and the photocatalytic properties of the formed Fe–Ag nanocomposites were studied.

2. Experimental part

In this work, silver (I) ferrite was synthesized by co-precipitation method using a modified procedure from [24]. Silver (I) nitrate (0.06 mol) and iron (III) nitrate (0.06 mol) were dissolved in 300 mL of distilled water of room temperature and stirred on a magnetic stirrer at 70°C for 1 h. The 2M aqueous sodium hydroxide solution was added dropwise to this mixture until pH 12 was reached, and it was stirred for 3 h. A ruby-red precipitate formed, which was filtered and washed with 150 mL of distilled water heated to 50°C. It was dried at 80°C to constant weight. The resulting reddish-brown powder was divided into 3 equal parts and thermally treated at 500°C, 700°C and 900ºC for 2 hours. The heat treated composites were ground in a Tube Mill control at the same speed and duration of grinding.

On this procedure, the composites of silver ferrite with polyvinyl alcohol (PVA) as a polymeric stabilizer of the particles were also fabricated, when metal salts were dissolved in the 3% PVA solution. The resulting precipitate was filtered and washed with distilled water of room temperature. After drying, the composite of silver ferrite precursors and PVA adsorbed on them was also thermally treated at 500°C, 700°C and 900°C for 2 hours.

The phase constitutions of heat treated silver ferrite samples, as well as the same samples after electrochemical reduction and after application in the electrohydrogenation of *p*- and *o*-nitrobenzoic acids were determined using a X-ray diffractometer (Bruker D8 ADVANCE ECO) using Cu-Kα radiation in the angle range (2θ) of 15-90°. Their morphological features were studied using a scanning electron microscope (TESCAN MIRA 3 LMU).

The electrocatalytic properties of formed Ag-Fe composites were studied in the electrohydrogenation of *p*- and *o*-nitrobenzoic acids, the main hydrogenation products of which were the corresponding isomers of aminobenzoic acid. The experiments were carried out in a diaphragm cell in an aqueous alkaline catholyte solution at a current of 1.5 A and temperature of 30°C in two stages: the electrochemical reduction of $AgFeO_2$ samples, and then the electrohydrogenation of NBA isomers. Silver (I) ferrite powder (weighing 1 g) was applied to a horizontally placed copper cathode (with an area of 0.05 dm^2) tightly adjacent to the bottom of the electrolytic cell. The $AgFeO_2$ powder, which has magnetic properties, was held on the cathode by an external magnet. The platinum gauze was served as an anode. Electrocatalytic hydrogenation of the organic compound on reduced metal composites was carried out after the termination of hydrogen absorption in the first stage. The initial concentrations of *p*- and *o*-NBA were 0.066 mol/L. Based on the volumes of gases (oxygen and hydrogen) evolved, the rate of the hydrogenation reaction (W, mL H_2/min), the hydrogen utilization coefficient (η, %), and the conversion of the reduced substance (α, %) were calculated.

3. Results and discussion

Bimetallic Fe-Ag composites were prepared on the basis of silver (I) ferrite. Silver ferrite was synthesized by co-precipitation method without and in the presence of the PVA polymeric stabilizer followed by heat treatment at 500, 700, and 900°C and electrochemical reduction.

Table 1 presents the weight losses of silver ferrite samples during heat treatment, their weights after heat treatment and the content of both metals in 1 g of each sample, calculated taking into account their amounts in the initial salts. With the same molar ratio of silver and iron salts taken for the silver ferrite synthesis, the silver content in 1 g of the samples is significantly higher than that of iron. The initial weights of silver ferrites without and with PVA were 3.55 g and 5.00 g, respectively. Despite the difference in the initial weights, the higher weight loss of the samples synthesized with PVA during heat treatment confirms the adsorption of the polymer on the particles of precipitated metal oxides as the precursors for the formation of silver ferrite.

Table 1 – Some characteristics of silver heat treated ferrite samples

Silver ferrite samples	The HT temperature, ºC	The weight loss during HT, g	Silver ferrite weight, g	Metals content in 1 g of silver ferrite, g	
				Ag	Fe
$AgFeO_2$	500	0.06	3.49	0.619	0.321
$AgFeO_2$	700	0.23	3.32	0.651	0.337
$AgFeO_2$	900	0.24	3.31	0.652	0.338
$AgFeO_2$ + PVA	500	1.29	3.71	0.582	0.302
$AgFeO_2$ + PVA	700	1.62	3.38	0.639	0.331
$AgFeO_2$ + PVA	900	1.65	3.35	0.645	0.334

For the prepared $AgFeO_2$ and $AgFeO_2$ + PVA samples, X-ray diffraction (XRD) analyses were performed. According to the XRD pattern of the $AgFeO_2$ sample heat-treated at 500°C (Figure 1, 1a), its phase constitution corresponds to the XRD data for silver ferrite with a rhombohedral crystal structure [7].

The particle sizes were calculated using the Scherer formula and X-ray diffraction data for prepared composites. The sizes of the silver ferrite particles of the (102) crystalline phase corresponding to the extended peak at the diffraction angle $2\theta = 35.30^o$ in the XRD pattern are ~ 9 nm. The particle sizes of other crystalline phases of this ferrite sample vary from 5.7 to 39 nm. Electron microscopic studies of this sample, indeed, show a fine-grained structure of its particles with a tight fit to each other (Figure 2).

According to XRD analysis (Figure 1, 2a), the heat treatment (HT) of silver ferrite at 700°C is accompanied by its decomposition into iron oxide (III) and silver metal (reaction equation (1)). This sample contains Ag and α-Fe_2O_3 crystalline phases. The size of the silver crystallites of the phase at the angle of $2\theta = 38.3°$ is ~16 nm. In the micrograph of this sample, taken with a BSE detector (Figure 2, b), it is clearly seen that multiple light inclusions of different sizes appear on the surface of its particles, corresponding to silver crystallites.

The $AgFeO_2$ sample (900°C) after HT (Figure 1, 3a) also contains silver and hematite (α-Fe_2O_3) in smaller amounts in its constitution. In addition to silver, the presence of reduced iron is also possible in this sample, the iron corresponding peaks are located along the peaks of silver in the XRD pattern. For example, for Fe, the values of 2θ angles for its main crystalline phases are 44.3°, 64.4°, 81.6°, and for Ag, they are 44.5°, 64.5° and 81.8°. The formation of alloyed Ag-Fe particles is also possible. It follows from the XRD data that all particles are large (40–80 nm). Micrographs show iron-containing crystalline formations up to several micrometers (Figure 2, c). The melted silver (see the attached spectrum of one of the light areas in micrograph (Figure 2, c)) covers these crystals in the form of films of different thicknesses.

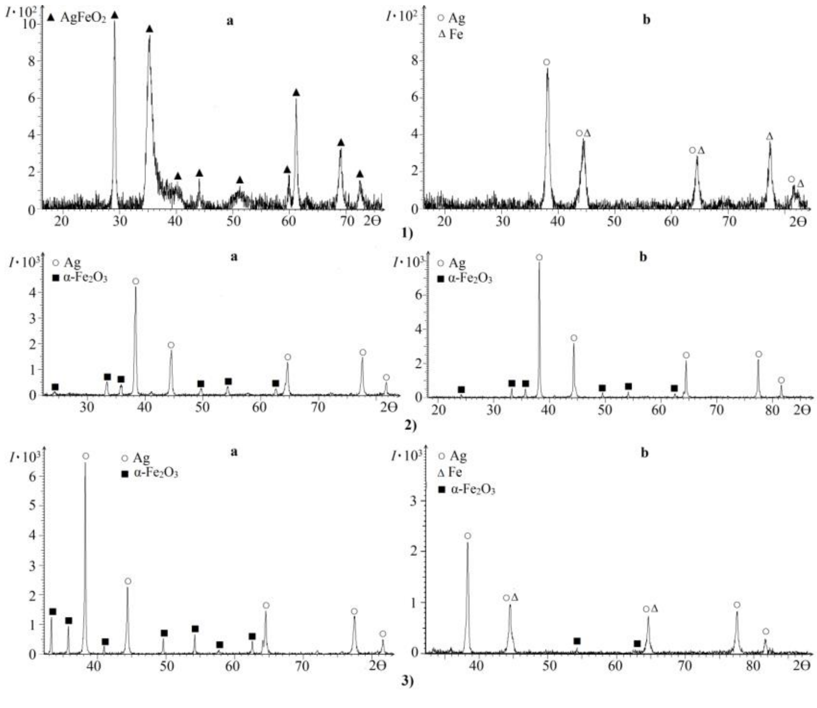

Figure 1 – XRD patterns of $AgFeO_2$ samples heat treated at 500°C (1), 700°C (2) and 900°C (3) after HT (a) and after electrochemical reduction and electrohydrogenation of NBA (b)

Note that the $AgFeO_2$ samples prepared without a polymeric stabilizer and treated at 700 and 900°C have magnetic properties, while the sample with HT at 500°C does not have such properties. This is in a good agreement with the results of the work [24], which states that silver ferrite annealed at 400°C is paramagnetic (remanent magnetization value M_R = 0.0023 emu/g). At the same time, composites fabricated from silver ferrite during heat treatment at 700 and 900°C exhibit ferromagnetic properties (M_R = 0.035 and 0.383 emu/g, respectively).

The phase constitutions of all three $AgFeO_2$ samples after electrochemical experiments are shown in Figure 1, 1b-3b. In the $AgFeO_2$ (500°C) sample, in which only silver ferrite particles were present after HT (Figure 1, 1a), the electrochemical reduction of silver cations and partially of iron cations occurs, when it is saturated with hydrogen. In the XRD pattern (Figure 1, 1b), the peaks for these metals are located together, and as noted above, the alloyed Ag-Fe particles (or heterostructural formations) could be formed. The $AgFeO_2$ (700°C) sample contains only crystalline phases of silver and iron oxide (α-Fe_2O_3). In the $AgFeO_2$ (900°C) sample, reduced iron appears in a small amount (Figure 1, 3b).

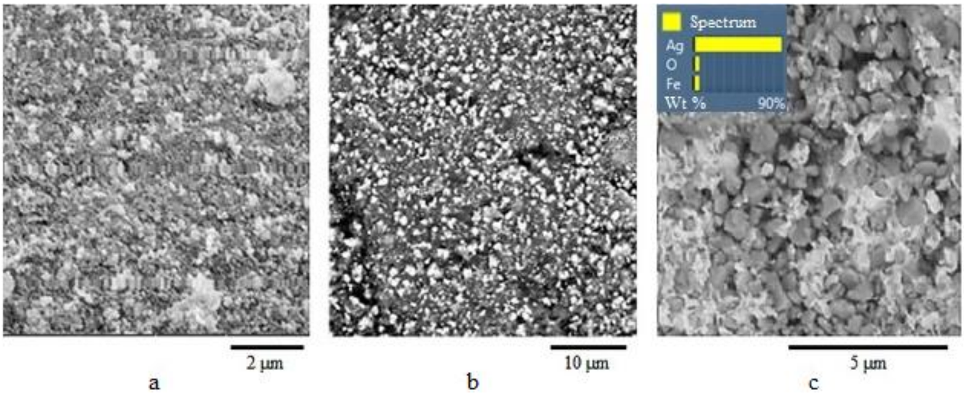

Figure 2 – Micrographs of $AgFeO_2$ samples heat treated at 500°C (a), 700°C (b) and 900°C (c)

The presence of the PVA polymer in the process of co-precipitation of metal cations affects the phase changes of silver ferrite samples during their heat treatment. So, already in the XRD pattern of the $AgFeO_2$ + PVA (500°C) sample (Figure 3, 1a), the peaks appear corresponding to the crystalline phases of metallic silver. The remaining silver ferrite and iron oxide α-Fe_2O_3 are also present. That is, under the action of temperature and PVA polymer, a partial decomposition of silver ferrite occurs at 500°C, which takes place at higher temperature in the case of $AgFeO_2$ prepared without the polymer (Figure 1).

The XRD pattern for $AgFeO_2$ + PVA (700°C) sample shows almost the same phase constitution (Figure 3, 2a) as for the sample annealed at 500°C, and obviously with a smaller number of silver ferrite phases.

In the $AgFeO_2$ + PVA (900°C) sample, in addition to the crystalline phases of metallic silver, iron and iron oxide α-Fe_2O_3, there is presumably another modification of this oxide, γ-Fe_2O_3 (maghemite), with low-intensity peaks in the X-ray diffraction pattern (Figure 3, 3a). It is known that the phase transition from γ-Fe_2O_3 to the more stable modification α-Fe_2O_3 occurs in the region of 550-560°C [28, 29], but during stabilization it can also exist at higher temperatures. Apparently, silver acts as its stabilizer in this heat-treated sample. At the same time, this sample exhibits weaker magnetic properties than the other two samples synthesized using the PVA polymer and treated at 500°C and 700°C.

From the micrographs of these samples, one can trace their morphological changes: from the beginning of the Ag particles separation from the rather dense $AgFeO_2$ structure to the formation of almost pure metallic Fe and Ag large crystals several micrometers in size (their compositions are shown in the EDS spectra 2 and 3, attached to the micrograph b) and to the sample with some melted silver (Figure 4, d).

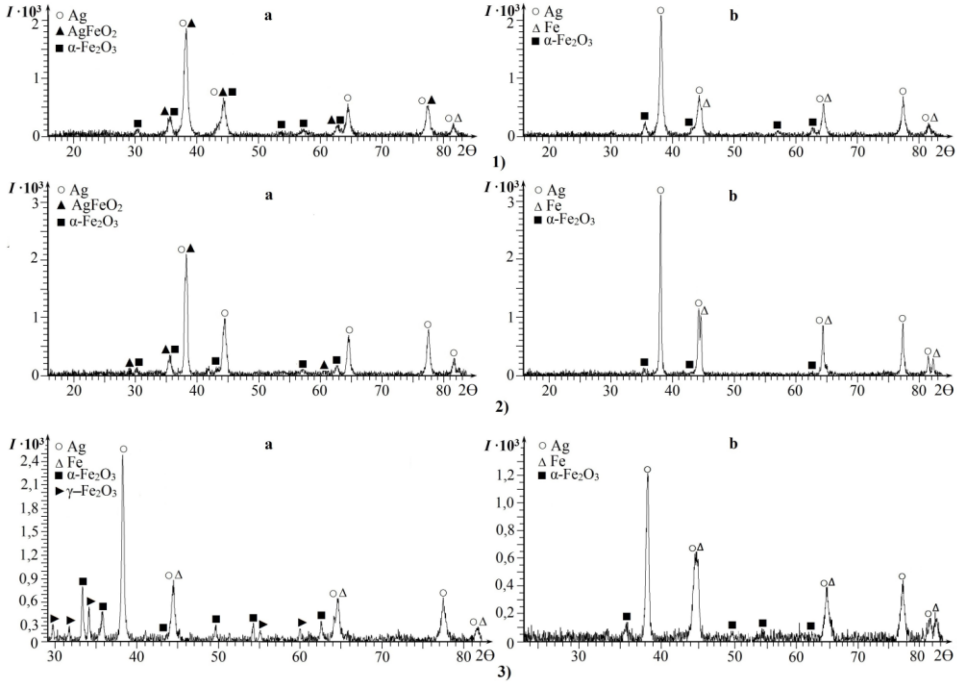

Figure 3 – XRD patterns of $AgFeO_2$ + PVA samples after heat treatment (a) at 500°C (1), 700°C (2) and 900°C (3) and after electrochemical reduction and NBA electrohydrogenation (b)

Heat-treated silver ferrite samples were deposited on the surface of a copper cathode, held on it with a magnet placed outside the cell, and saturated with hydrogen. Then the resulting Ag-Fe composites were investigated for the manifestation of electrocatalytic activity in the electrohydrogenation of *p*- and *o*-isomers of nitrobenzoic acid (*p*- and *o*-NBA). The obtained results are shown in Table 2.

It should be noted that the electrochemical reduction of aromatic nitro compounds, as a rule, is complicated by the various chemical transformations of the intermediate reduction products formed and significantly depends on the pH of the environment [30]. The electrocatalytic hydrogenation of nitro compounds proceeds by the mechanisms similar to their catalytic hydrogenation on heterogeneous catalysts in the liquid phase. Brief reviews of the catalytic hydrogenation processes of nitroarenes with a description of their mechanisms can be found in recently published articles [31, 32].

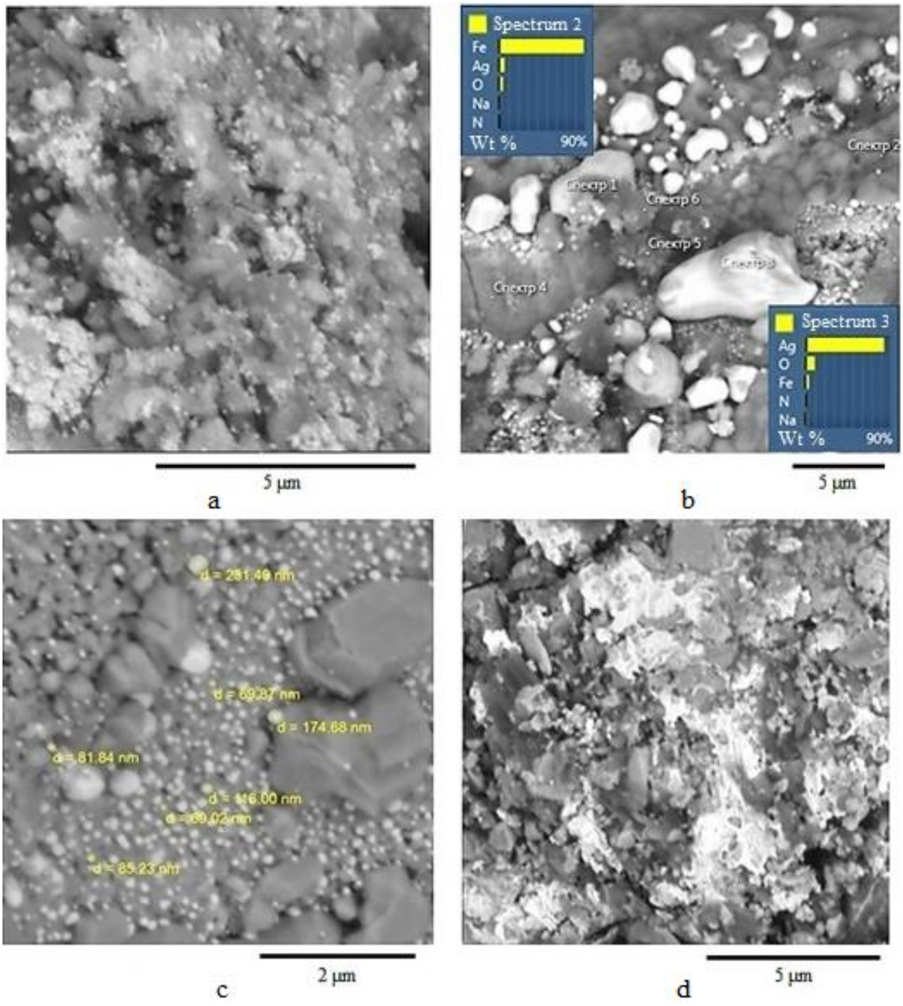

a b

c d

Figure 4 – Micrographs of $AgFeO_2$ +PVA samples annealed at 500°C (a), 700°C (b and c) and 900°C (d)

From the data in Table 2 it follows that all heat-treated $AgFeO_2$ samples absorb hydrogen and undergo an electrochemical reduction, but to variable degrees, which are determined by changes in their phase constitutions that occur during heat treatment at different temperatures. The $AgFeO_2$ (500°C) sample after HT practically retains the silver ferrite crystal structure (Figure 1, 1a), therefore, in the electrochemical system, its reduction is accompanied by the absorption of the largest volumes of hydrogen (131.1 and 125.2 mL H_2). For the complete reduction of silver and iron cations from 1 g of $AgFeO_2$ taken to activate the Cu cathode, according to the equation

$$AgFeO_2 + 4e^- + 4H^+ \rightarrow Ag^0 + Fe^0 + 2H_2O, \qquad (2)$$

228 mL of H_2 are needed, of which 57 mL are used to reduce of silver cations, and 171 mL for the reduction of iron cations. Obviously, in the $AgFeO_2$ (500°C) sample, all the silver and part of the iron cations are reduced. In all other $AgFeO_2$ and $AgFeO_2$ + PVA samples, two metals are partially formed even during their heat treatment both during the release of oxygen from $AgFeO_2$ and as a result of reduction by PVA decomposition products. Therefore, in the electrochemical system, they absorb smaller volumes of hydrogen.

Table 2 – The results of the electrochemical reduction of silver ferrite samples and electrocatalytic hydrogenation of *p*-NBA and *o*-NBA

Silver ferrite samples	Electrochemical reduction of $AgFeO_2$		Electrocatalytic hydrogenation of NBA's		
	τ, min	V_{H2}, mL	*W*, mL H_2/min ($\alpha = 0.25$)	η, %	α, %
p-Nitrobenzoic acid					
Cu cathode	-	-	3.7	36.1	63.9
$AgFeO_2$ (500°C)	80	131.1	9.0	88.9	99.4
$AgFeO_2$ (700°C)	20	17.0	6.3	61.5	93.5
$AgFeO_2$ (900°C)	60	98.1	9.3	90.3	100.0
$AgFeO_2$ + PVA (500°C)	20	30.2	9.5	91.7	97.2
$AgFeO_2$ + PVA (700°C)	30	38.7	8.6	83.3	94.6
$AgFeO_2$ + PVA (900°C)	60	46.9	8.4	81.9	96.0
o-Nitrobenzoic acid					
Cu cathode		-	3.8	36.1	66.4
$AgFeO_2$ (500°C)	60	125.2	7.9	77.8	99.6
$AgFeO_2$ (700°C)	50	25.8	7.0	67.8	99.9
$AgFeO_2$ (900°C)	40	88.7	9.3	91.7	99.3
$AgFeO_2$ + PVA (500°C)	30	38.6	9.1	88.9	99.8
$AgFeO_2$ + PVA (700°C)	30	38.6	8.5	83.3	99.5
$AgFeO_2$ + PVA (900°C)	40	51.4	9.0	87.5	99.8

The electrocatalytic hydrogenation of both NBA isomers in the presence of Fe–Ag composites formed after the electrochemical reduction of thermally treated silver ferrite samples proceeds noticeably faster than their electrochemical reduction on a Cu cathode (Table 2). Moreover, more consistently high conversion values are repeated for all samples in the case of electrocatalytic hydrogenation of *o*-NBA. In general, it is quite difficult to determine, electrocatalytic hydrogenation of which NBA isomer is more intense using the prepared Fe–Ag composites, since high hydrogenation rates (9.3–9.5 mL H_2/min) are achieved in processes of both NBA isomers being studied. It can be noted that composites containing crystalline phases of two metals or their alloys after electrochemical reduction are electrocatalytically more active than composites containing only reduced silver and iron oxide α-Fe_2O_3.

4. Conclusion

Thus, the performed experiments have established that silver ferrite $AgFeO_2$ can be reduced in the electrochemical system under specified conditions, and the degree of its reduction is determined by changes in the phase constitution of $AgFeO_2$ samples during preliminary heat treatment. The resulting Fe–Ag composites exhibit a high electrocatalytic activity in the electrohydrogenation of *p*- and *o*-nitrobenzoic acids and, obviously, can be used as catalysts in the synthesis of other aminocompounds.

Funding: The research was carried out with the financial support of the Science Committee of the Ministry of Education and Science of the Republic of Kazakhstan (the scientific and technical Program № BR10965230).

Conflict of interest: The authors declare that they have no conflict of interest.

БИМЕТАЛДЫ Fe-Ag КОМПОЗИТТЕРІНІҢ ҚОЛДАНЫЛУЫМЕН НИТРОБЕНЗОЙ ҚЫШҚЫЛЫНЫҢ *п*- ЖӘНЕ *о* -ИЗОМЕРЛЕРІН ЭЛЕКТРКАТАЛИЗДІК ГИДРЛЕУ

***Е.А. Соболева*[1*], *Я.А. Висурханова*[1,2], *Н.М. Иванова*[1], *М.Е. Бейсенбекова*[1], *С.О. Кенжетаева*[2]**

[1]*ЖШС «ҚР Органикалық синтез және көмір химиясы институты», Қарағанды, Қазақстан*
[2] *КЕАҚ «Академик Е.А.Бөкетов атындағы Қарағанды университеті», Қарағанды, Қазақстан*
E-mail: esoboleva-kz@mail.ru

Түйіндеме. Биметалды Fe-Ag композиттері, нанобөлшектердің тұрақтандырғышы ретінде поливинил спиртінің (ПВС) қатысуысыз және оның қатысуымен бірге тұндыру әдісімен синтезделген, күміс (І) ферриті ($AgFeO_2$) негізінде, соңынан оны 500, 700 және 900° С температурада термиялық өңдеу (ТӨ) және электрохимиялық тотықсыздандыру арқылы алынды. Термиялық өңдеуден кейін және электрохимиялық эксперименттерден кейін алынған $AgFeO_2$ үлгілерінің фазалық құрамдары рентгенфазалық талдау және электронды микроскопия әдістерімен анықталды және морфологиялық ерекшеліктері зерттелді. Поливинил спиртімен дайындалған күміс ферритінің термиялық ыдырау температурасының төмендегені анықталды. Сулы-сілтілі католитте мыс катодында екі металлдың немесе олардың құймасының кристалдық фазалары түзілуімен жүретін $AgFeO_2$ электрохимиялық тотықсыздану мүмкіндігі көрсетілді. Термиялық өңдеу және электрохимиялық тотықсыздану барысында қалыптасатын Fe-Ag композиттері нитробензой қышқылының *п*- және *о*-изомерлерін электргидрлеу үрдістерінде электркатализаторлар ретінде қолданылды және жоғары белсенділік көрсетті. Олардың электрохимиялық тотықсыздануымен салыстырғанда, тура осындай жағдайларда гидрлену жылдамдығы және сутекті қолдану коэффициенті артты, ал олардың конверсиясы максималды шамаларға жетті. Электркатализдік гидрленудің негізгі өнімдері дәрілік препараттар (мысалы, анестезин, новокаин ж.б.) өндірісінде кеңінен қолданылатын аминобензой қышқылының *п*- және *о*-изомерлері болып табылады.

Түйін сөздер: биметалдық Fe-Ag композиттері, күміс ферриті, полимерді тұрақтандырғыш, электркатализдік гидрлеу, нитробензой қышқылының п- және о-изомерлері

Соболева Елена Анатольевна	*Химия ғылымдарының кандидаты*
Висурханова Яха Амхадовна	*PhD студент*
Иванова Нина Михайловна	*Химия ғылымдарының докторы, профессор*
Бейсенбекова Молдир Ерболатовна	*Техника және технологиялар бакалавры*
Кенжетаева Сауле Орынбаевна	*Химия ғылымдарының кандидаты*

ЭЛЕКТРОКАТАЛИТИЧЕСКОЕ ГИДРИРОВАНИЕ *п*- И *о* -ИЗОМЕРОВ НИТРОБЕНЗОЙНОЙ КИСЛОТЫ С ПРИМЕНЕНИЕМ БИМЕТАЛИЧЕСКИХ Fe-Ag КОМПОЗИТОВ

Е.А. Соболева[1*], Я.А. Висурханова[1,2], Н.М. Иванова[1], М.Е. Бейсенбекова[1], С.О. Кенжетаева[2]

[1]ТОО «Институт органического синтеза и углехимии РК», Караганда, Казахстан
[2]НАО «Карагандинский университет имени академика Е.А. Букетова», Караганда, Казахстан
E-mail: esoboleva-kz@mail.ru

Резюме. Биметаллические Fe-Ag композиты получены на основе феррита серебра (I) ($AgFeO_2$), синтезированного методом соосаждения без и в присутствии поливинилового спирта, как стабилизатора наночастиц, с последующей термической обработкой при 500, 700 и 900^{o}C и электрохимическим восстановлением. Методами рентгенофазового анализа и электронной микроскопии определены фазовые составы и изучены морфологические особенности полученных образцов $AgFeO_2$ после термической обработки и после электрохимических экспериментов. Установлено снижение температуры термического распада феррита серебра, приготовленного с поливиниловым спиртом. Показана возможность электрохимического восстановления $AgFeO_2$ в водно-щелочном католите на медном катоде с образованием кристаллических фаз обоих металлов или их сплава. Формирующиеся в ходе термической обработки и электрохимического восстановления Fe-Ag композиты были применены в качестве электрокатализаторов в электро-гидрировании *п*- и *о*-изомеров нитробензойной кислоты и проявили высокую активность. По сравнению с их электрохимическим восстановлением в аналогичных условиях повысились скорость гидрирования и коэффициент использования водорода, а их конверсия достигла максимальных значений. Основными продуктами электрокаталитического гидрирования являются *п*- и *о*-изомеры аминобензойной кислоты, широко применяемые в производстве лекарственных препаратов (например, анестезина, новокаина и др.).

Ключевые слова: биметаллические Fe-Ag композиты, феррит серебра, полимерный стабилизатор, электрокаталитическое гидрирование, *п*- и *о*-изомеры нитробензойной кислоты

Соболева Елена Анатольевна	*Кандидат химических наук*
Висурханова Яха Амхадовна	*PhD студент*
Иванова Нина Михайловна	*Доктор химических наук, профессор*
Бейсенбекова Молдир Ерболатовна	*Бакалавр техники и технологий*
Кенжетаева Сауле Орынбаевна	*Кандидат химических наук, профессор*

References

1. Kharissov B.I., Dias H.V.R., Kharissova O.V. Mini-review: Ferrite nanoparticles in the catalysis. *Arabian J. Chem.* **2019**, *12*, 1234-1246. DOI: org/10.1016/j.arabjc.2014.10.049
2. Sanadi K.R., Kamble G.S. Novel synthesis of silver ferrite by sol–gel auto combustion method and study of its photocatalytic activity. *Adv. Porous Mater*. **2017**, *5*, 1-4. DOI: 10.1166/apm.2017.1148

3. Hosseini S.M., Hosseini-Monfared H., Abbasi V. Silver ferrite-graphene nanocomposite and its good photocatalytic performance in air and visible light for organic dye removal. *Appl. Organometal. Chem*, **2016**, *31*, No 4, 1-8. DOI: 10.1002/aoc.3589

4. Yin L., Shi Y., Lu L., Fang R., Wan X., Shi H. A Novel delafossite structured visible-light sensitive $AgFeO_2$ photocatalyst: preparation, photocatalytic properties, and reaction mechanism. *Catalysts*, **2016**, *6*, No 5, 69. DOI: 10.3390/catal6050069

5. Shi Z., Wang T., Lin H., Wang X., Ding J., Shao M. Excellent surface-enhanced Raman scattering (SERS) based on $AgFeO_2$ semiconductor nanoparticles. *Nanoscale*, **2013**, *5*, No 20, 10029-10033. DOI: 10.1039/c3nr03460g

6. Durham J.L., Kirshenbaum K., Takeuchi E.S., Marschilok A.C., Takeuchi K.J. Synthetic control of composition and crystallite size of silver ferrite composites profound electrochemistry impacts. *Chem. Comm*, **2015**, *51*, No 24, 5120-5123. DOI: 10.1039/c4cc10277k

7. Farley K.E., Marschilok A.C., Takeuchi E.S., Takeuchi K.J. Synthesis and electrochemistry of silver ferrite. *Electrochem. Solid State Lett.*, **2011**, *15*, No 2, A23-A27. DOI: 10.1149/2.010202esl

8. Marquardt M.A., Ashmore N.A., Cann D.P. Crystal chemistry and electrical properties of the delafossite structure. *Thin Solid Films,* **2006**, *496*, No 1, 146-156. DOI: 10.1016/j.tsf.2005.08.316

9. Zhao Y., An H., Feng J., Ren Y., Ma J. Impact of crystal types of $AgFeO_2$ nanoparticles on the peroxymonosulfate activation in the water. *Environ. Sci. Technol.*, **2019**, *53*, No 8, 4500-4510. DOI: 10.1021/acs.est.9b00658

10. Abdelhamid H.N., Wu H.F. Facile synthesis of nano silver ferrite ($AgFeO_2$) modified with chitosan applied for biothiol separation. *Mater. Sci. Eng.*, **2014**, *45*, 438-445. DOI: 10.1016/j.msec.2014.08.071

11. Abdelhamid H.N., Talib A., Wu H.-F. Facile synthesis of water soluble silver ferrite ($AgFeO_2$) nanoparticles and their biological application as antibacterial agents. *RSC Adv*., **2015**, *5*, 34594-34602. DOI: 10.1039/C4RA14461A

12. Sobolev A., Rusakov V., Moskvin A., Gapochka A., Belik A., Glazkova I., Akulenko A., Demazeau G., Presniakov I. 57Fe Mössbauer study of unusual magnetic structure of multiferroic 3R-$AgFeO_2$. *J. Phys.: Condens. Matter,* **2017**, *29,* No 27, 275803. DOI: 10.1088/1361-648X/aa70ae

13. Brollo M., López-Ruiz R., Muraca D. Figueroa S.J.A., Pirota K.R., Knobel M. Compact Ag@Fe_3O_4 core-shell nanoparticles by means of single-step thermal decomposition reaction. *Sci. China Chem*., **2014**, *4*, 6839. DOI: 10.1038/srep06839

14. Dong Yu., Yang Z., Sheng Qu., Zheng J. Solvothermal synthesis of $AgFe_3O_4$ nanosphere and its application as hydrazine sensor. *Colloids Surf. A,* **2018**, *538*, No 2, 371-377. DOI: 10.1016/j.colsurfa.2017.11.024

15. Angotzi M.S., Mameli V., Cara C., Grillo V., Enzo S., Musinu A., Cannas C. Defect-assisted synthesis of magneto-plasmonic silver-spinel ferrite heterostructures in a fower-like architecture. *Sci. Rep*., **2020**. *10*, No 1, 17015. DOI: 10.1038/s41598-020-73502-5

16. Gomes G.A., Costa G.L., Silva Figueiredo A.B. Synthesis of ferrite nanoparticles $Cu_{1-x}Ag_xFe_2O_4$ and evaluation of potential antibacterial activity. *J. Mater. Res. Technol*., **2018**, *7*, No 3, 381-386. DOI: 10.1016/j.jmrt.2018.04.021

17. Satheeshkumar M.K., Kumar E.R., Srinivas Ch., Suriyanarayanan N., Deepty M., Prajapat C.L., Chandrasekhar Rao T.V., Sastry D.L. Study of structural, morphological and magnetic properties of Ag substituted cobalt ferrite nanoparticles prepared by honey assisted combustion method and evaluation of their antibacterial activity. *J. Magn. Magn. Mater*, **2019**, *469*, 691-697. DOI: 10.1016/j.jmmm.2018.09.039

18. Jiaowen S., Kim D.W., Kim S.B., Jo Y.M. CO_2 decomposition using metal ferrites prepared by co-precipitation method. *Korean J. Chem. Eng*., **2016**, *33*, 3162-3168. DOI: 10.1007/s11814-016-0192-5

19. Kazemi M., Sichen D. Investigation of selective reduction of iron oxide in zinc ferrite by carbon and hydrogen. *J. Sustain. Metall.*, **2016**, *2*, 73-78. DOI: 10.1007/s40831-015-0037-1

20. Junca E., Grillo F.F., Restivo T.A.G., Tenorio J.A.S. Kinetic investigation of synthetic zinc ferrite reduction by hydrogen. *J. Thermal Anal. Calorim*., **2017**, *129*, 6222-6227. DOI: 10.1007/s10973-017-6222-7

21. Ivanova N.M., Soboleva E.A., Visurkhanova Ya.A., Muldakhmetov Z. Electrochemical synthesis of Fe–Cu composites based on copper(II) ferrite and their electrocatalytic properties. *Russ. J. Electrochem*., **2020**, *56*, 533-543. DOI: 10.1134/S1023193520070034

22. Vissurkhanova Ya.A., Soboleva E.A., Ivanova N.M., Muldakhmetov Z.M. Thermal and electrochemical reduction of nickel (II) ferrite under the influence of polymer stabilizers. *Bulletin of the Karaganda University Chemistry Series*, **2020**, No 2 (98), 42-50. http://doi.org/10.31489/2020Ch2/42-50.

23. Ivanova N.M., Muldakhmetov Z.M., Soboleva E.A., Vissurkhanova Ya.A., Beisenbekova M.E. Thermal and electrochemical reduction of zinc ferrite doped with polymer. *Electrochem. Comm*., **2021**, *128*. Available at: https://doi.org/10.1016/j.elecom.2021.107070.

24. Murthy Y.L.N., Rao T.K., Kasiviswanath I.V., Singh R. Synthesis and characterization of nano silver ferrite composite. *J. Magn. Magn. Mater,* **2010**, *322,* 2071-2074. DOI: 10.1016/j.jmmm.2010.01.036

25. Gayen R.N., Laha P. Single-step synthesis and optical properties of bimetallic Fe-Ag nanoparticles. *J. Nanosci. Nanotechnol*., **2017**, *17,* No 1, 666-670. DOI: 10.1166/jnn.2017.12389

26. Vural M., Crowgey B., Kempel L.C., Kofinas P. Nanostructured flexible magneto-dielectrics for radio frequency application. *J. Mater. Chem. C*, **2014**, *2*, 756-763. DOI: 10.1039/C3TC32113D

27. Sridharan K., Endo T., Cho S.-G., Kim J., Park T.J., Philip R. Single step synthesis and optical limiting properties of Ni-Ag and Fe-Ag bimetallic nanoparticles. *Optical Materials*, **2013**, *35*, 860-867. DOI: 10.1016/j.optmat.2012.10.053

28. Ye X., Lin D., Jiao Z., Zhang L. The termal stability of nanocrystalline maghemite Fe_2O_3. *J. Phys. D. Appl. Phys*., **1998**, *31*, 2739-2744. DOI: 10.1088/0022-3727/31/20/006

29. Kazeminezhad I., Mosivand S. Phase transition of electrooxidized Fe_3O_4 to γ and α-Fe_2O_3 nanoparticles using sintering treatment. *Acta Physica Polonica A*, **2014**, *125*, 1210-1214. DOI: 10.12693/APhysPolA.125.1210

30. Tomilov A.P., Fioshin M.Ya., Smirnov V.A. *Elektrokhmicheskii sintez organicheskikh veshchestv* [Electrochemical synthesis of organic substances]. Leningrad, Khimiya, 1976, 423 p.

31. Mali M. Highly selective catalytic reduction of nitroarenes over heterogeneous transition metal catalysts: Nano-catalysts – the new challenges. *Synth. Catal.*, **2017**, *2*, 8 p. DOI: 10.4172/2574-0431.100014

32. Song J., Huang Z.-F., Pan L., Li K., Zhang X., Wang L., Zou J.-J. Review on selective hydrogenation of nitroarene by catalytic, photocatalytic and electrocatalytic reactions. *Appl. Catal. B: Environmental*, **2018**, *227*, 386-408. DOI: 10.1016/j.apcatb.2018.01.052